Double Diffusive Natural Convection in a Nuclear Waste Repository

Yue Hao, John J. Nitao, Thomas A. Buscheck, and Yunwei Sun
L-631, Lawrence Livermore National Laboratory, Livermore, CA 94551

Abstract – *In this study, we conduct a two-dimensional numerical analysis of double diffusive natural convection in an emplacement drift for a nuclear waste repository. In-drift heat and moisture transport is driven by combined thermal- and compositional-induced buoyancy forces. Numerical results demonstrate buoyancy-driven convective flow patterns and configurations during both repository heat-up and cool-down phases. It is also shown that boundary conditions, particularly on the drip-shield surface, have strong impacts on the in-drift convective flow and transport.*

I. INTRODUCTION

It is recognized that natural convection plays an important role in many heat and mass transfer processes. In nonisothermal applications with binary fluid mixtures, the interaction of natural heat convection with mass transport of two components results in a complex flow and transport phenomenon called double diffusive convection. Double diffusive convection, resulting from buoyancy forces caused by temperature and compositional gradients, is found in many natural-system and engineering applications. For this reason it has attracted considerable attention [1, 2]. One potential example is related to the transport of heat and moisture inside emplacement drifts in a nuclear-waste repository in the unsaturated zone. After the emplacement of waste packages, the radioactive heat of decay generates water vapor due to the evaporation of water in the adjoining host rock, which migrates into the drift. Within the drift, natural convection contributes to transport of water vapor from hotter to cooler locations, where it may condense.

In addition to affecting heat and mass transport, the complicated flow patterns and structures induced by combined thermal and compositional buoyancy effects will influence evaporation and condensation on engineered material surfaces within the drift. Because of the potential for influencing the corrosion of drip shields and waste packages, moisture condensation within drifts is of concern for total system performance assessment of the repository. Moreover, analyses of in-drift heat and moisture convection can provide a better understanding of the basic physics of flow and transport phenomena inside engineered tunnels. Recent CFD models that apply the FLUENT code have been used to describe in-drift flows, with a focus on thermal-induced natural convection and determining effective dispersion coefficients for models predicting moisture transport and condensation [3, 4].

The goal of this work is to investigate double-diffusive convection inside an emplacement drift, using a Navier-Stokes model approach to examine and capture the predominant convection modes.

II. MATHEMATICAL FORMULATION

In this study, natural heat and mass convection in an air/vapor binary system is considered, using Navier-Stokes equations. The governing equations are expressed in the following mass, momentum, energy, and vapor concentration conservation forms:

Continuity:

$$\frac{\partial \rho}{\partial t} + \nabla \cdot (\rho \mathbf{u}) = 0 \tag{1}$$

Momentum:

$$\rho\left(\frac{\partial \mathbf{u}}{\partial t} + \mathbf{u} \cdot \nabla \mathbf{u}\right) = -\nabla p + \nabla \cdot \boldsymbol{\tau} + \rho \mathbf{g} \tag{2}$$

where t, ρ, $\mathbf{u}$, p, and $\mathbf{g}$ represent time, binary mixture density, velocity, pressure, and body force, and $\boldsymbol{\tau}$ is the viscous stress tensor,

$$\boldsymbol{\tau} = \mu\left[\nabla \mathbf{u} + (\nabla \mathbf{u})^T\right] \tag{3}$$

in which μ is fluid viscosity and the superscript T denotes the transpose.

Energy:

$$\rho C_p\left(\frac{\partial T}{\partial t} + \mathbf{u} \cdot \nabla T\right) = \nabla \cdot (k \nabla T) + Q \tag{4}$$

with T, C_p, k, and Q as temperature, specific heat, thermal conductivity, and heat generation term.

Vapor concentration (expressed as mass fraction) in a vapor-air mixture:

$$\rho\left(\frac{\partial C}{\partial t} + \mathbf{u} \cdot \nabla C\right) = \nabla \cdot (\rho D \nabla C) + R \tag{5}$$

C, D, and R are vapor mass fraction, binary diffusion coefficient, and vapor source term, respectively.

For this study, the total pressure of the air/vapor mixture p_∞ is assumed spatially uniform, and the binary mixture obeys the ideal gas law. Based on these conditions, the fluid density can be expressed as

$$\rho = \frac{p_\infty}{RT\left(\frac{C}{M_V} + \frac{1-C}{M_A}\right)} \tag{6}$$

with T as temperature, R as universal gas constant, M_V as molecular mass of water vapor and M_A as molecular mass of air.

If both temperature and vapor-concentration variations are small, then the Boussinesq approximation is applied with the fluid density simplified as

$$\rho = \rho_\infty[1 - \beta_T(T - T_\infty) - \beta_C(C - C_\infty)] \qquad (7)$$

in which subscript ∞ denotes the reference state, and β_T and β_C are the thermal and concentration expansion coefficients, respectively,

$$\beta_T = -\frac{1}{\rho}\left(\frac{\partial \rho}{\partial T}\right)_p \qquad \beta_C = -\frac{1}{\rho}\left(\frac{\partial \rho}{\partial C}\right)_p \qquad (8)$$

For thermal natural convection, we use the dimensionless Rayleigh number

$$Ra_T = \frac{g\beta_T \Delta T L^3}{\nu\alpha}$$

and Prandtl number

$$\mathrm{Pr} = \frac{\nu}{\alpha}$$

For mass transfer, we use the corresponding Rayleigh number

$$Ra_C = \frac{g\beta_C \Delta C L^3}{\nu D}$$

and Schmidt number

$$Sc = \frac{\nu}{D}$$

Here ΔT, ΔC, υ, α, and L are temperature difference, vapor-concentration difference, fluid kinematics viscosity, thermal diffusivity, and length scale, respectively.

In order to compare the magnitudes of thermal- and compositional-induced natural convections, the so called "buoyancy ratio" is introduced by [5],

$$\mathbf{N} = \frac{\beta_C \Delta C}{\beta_T \Delta T} \qquad (9)$$

The dominant driving buoyant force is determined by the buoyancy ratio N. It is obvious that as N decreases, thermal buoyancy effects will become dominant over compositional effects. The k–ω turbulent model [6] is used to account for turbulent flow effects for large Rayleigh-number problems. The above governing equations are solved by the Navier-Stokes module implemented in the NUFT code [7], which has been validated against benchmark problems.

III. RESULTS AND DISCUSSION

This study addresses both heat and vapor transport within an emplacement drift (Fig 1a). As depicted in Fig. 1b, the drip shield and waste package are lumped together as a monolithic heat source that is impermeable with respect to mass transport. We model a two-dimensional in-drift flow domain (Fig. 1a), which is bounded by the outer drip-shield surface, upper invert surface, and drift-wall surface above the invert. Due to the symmetry of the problem, only half of the drift needs to be represented in the numerical model (Fig. 1b).

For the problem shown in Fig. 1, in-drift flow and transport processes are highly dependent on thermal-hydrological conditions in the adjoining porous host rock. Hence the key aspect of modeling of in-drift flow is the specification of boundary conditions on the interfaces between the free/open-flow system in the drift and the porous-flow system in the host rock. Ideally one would determine these conditions by directly coupling free/open flow with porous flow. However, this is beyond the scope of the current study. For the purpose of this study, we assign appropriate boundary conditions on the surfaces of the drift wall, invert, and drip shield on the basis of results from the Multiscale Thermohydrologic Model (MSTHM) [8, 9, 10]. The MSTHM, which is based on porous-medium Darcy-flow approximations, predicts the coupled thermal-hydrological conditions at both drift-scale and mountain-scale. Fig. 2 plots the time history of the representative drift-wall temperature and vapor concentration obtained from the MSTHM LDTH-submodel simulations.

During the initial 50-year preclosure ventilation period, the heat generated by waste packages is removed by forced convective cooling. After drift ventilation ceases, the postclosure period begins and the drift-wall temperature abruptly rises (Fig. 2a) to well above the local boiling point of water (96°C). The vapor concentration at the drift-wall surfaces also sharply increases along with temperatures (Fig. 2b). The dryout phase lasts over 1000 years until the drift wall cools down to 96°C (Fig. 2b).

For simplicity, the temperature T_{dw}, T_{invert}, and T_{ds} are uniformly imposed along the drift-wall surface, upper invert surface, and drip-shield surface (Fig. 1b). In addition, the surfaces of the drift wall and invert are assumed to be permeable with constant vapor concentrations C_{dw} and C_{invert}. In order to explore all the possible flow patterns and convection modes inside the drift, we investigate two possible conditions on the outer drip-shield surface with respect to mass transfer.

The simulated transient behavior discussed in the following sections is not intended to be exactly representative of a real repository system. The primary purpose of this study is to illustrate the influence of boundary conditions on double diffusive natural convection within emplacement drifts, with a focus on the interaction between the thermal and compositional buoyancy forces. These simulations neglect phase change (evaporation and condensation) within the drift. Moreover, the transient aspects of the simulated behavior are presented to illustrate the interaction between the thermal and compositional buoyancy forces.

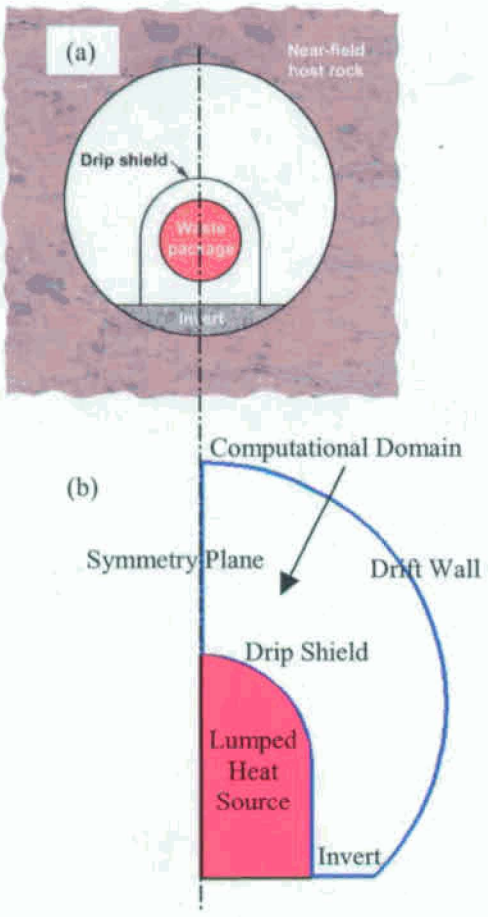

Fig. 1. (a) Schematic of the problem and (b) conceptual model are shown. Note that the drip shield and waste package are lumped together as a monolithic heat source.

III A. Zero Mass-Flux Condition on Drip-Shield Surface during Heat-Up and Cool-Down Phases

In this case the dry condition is maintained with no evaporation or condensation on the impermeable drip-shield surface. Therefore, the drip shield is subject to zero mass flux boundary condition

$$\left.\frac{\partial C}{\partial \mathbf{n}}\right|_{ds} = 0$$

with $\mathbf{n}$ as the unit normal to the drip-shield surface.

Based on MSTHM results [8, 10], the boundary vapor concentrations are fixed along the drift wall and invert surface. MSTHM results are also used to fix the boundary temperatures around the perimeter of the drift cavity, which includes the outer drip-shield surface, upper invert surface, and drift-wall surface above the top of the invert. Numerical examples are selected for two specific points in the thermal evolution of the repository system, one during the heat-up phase and the other during the cool-down phase (Fig. 2).

Fig. 3 plots temperature, flow velocity, and vapor concentration at different stages of the simulated transient flow development at $t = 52$ yr, which is during the heat-up phase. At this phase in the thermal evolution, temperature rise in the host rock has driven water vapor from the host rock into the drift. The opposing temperature and vapor-concentration gradients lead to countercurrent flows in the drift, as is evident in Fig. 3b, with upward thermal-induced buoyancy effects balanced by vapor movements. During the early stage of transient flow development (Fig. 3a), the buoyancy ratio $N > 1$. Thus, the compositional-induced buoyancy effect dominates inside the drift, where strong vapor fluxes suppress thermal natural convection. As vapor continues to flow into and mix within the drift, vapor concentration in the drift begins to approach that in the host rock, which reduces vapor flux into the drift. As the vapor concentration gradient decreases, the magnitude of the compositional driving force decreases to that of the thermal driving force ($N \sim 1$). Because they are of the same magnitude, there is more interaction between the two driving forces, resulting in more complex, unsteady countercurrent flow patterns (Fig. 3b).

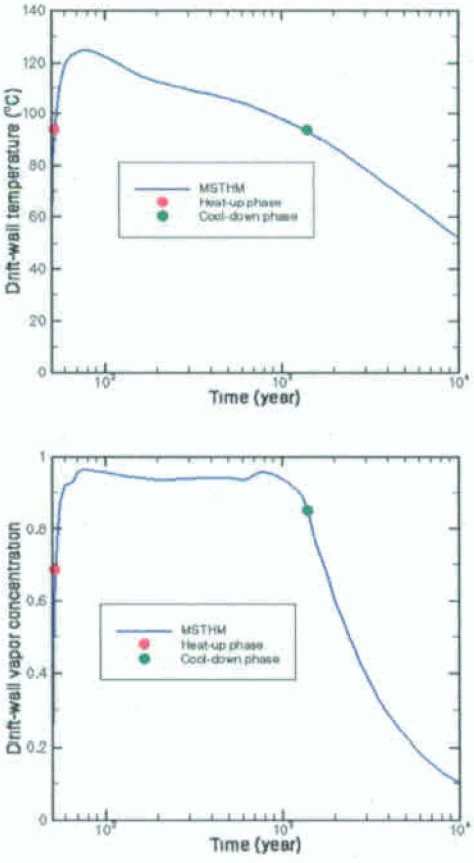

Fig. 2. The boundary conditions are obtained from the MSTHM LDTH submodel [8, 10] for two different phases in the thermal evolution of the repository.

As the vapor concentration in the drift approaches that in the host rock, vapor-concentration equilibrium is established between the drift and host rock. Moreover, the vapor-concentration gradient is diminished within the drift (Fig. 3c), causing flow to be dominated by thermal natural convection (N < 1). At this point, steady-state heat flow has been established in the drift.

When the repository cools down, water vapor leaves the drift, either by transport into the host rock or by condensation on the surfaces in the drift cavity. In this example, the temperature and concentration gradients are in the same direction. Therefore, the resulting thermal and compositional buoyancy effects induce a large upward circulation inside the drift, which is particularly strong during the early transient stage (Fig. 4a). During the intermediate stage, the flow magnitude is reduced along with the vapor-concentration gradient (Fig. 4b). As steady state is approached, the compositional buoyancy effects are minimal because the vapor-concentration distribution is uniform within the drift (Fig. 4c).

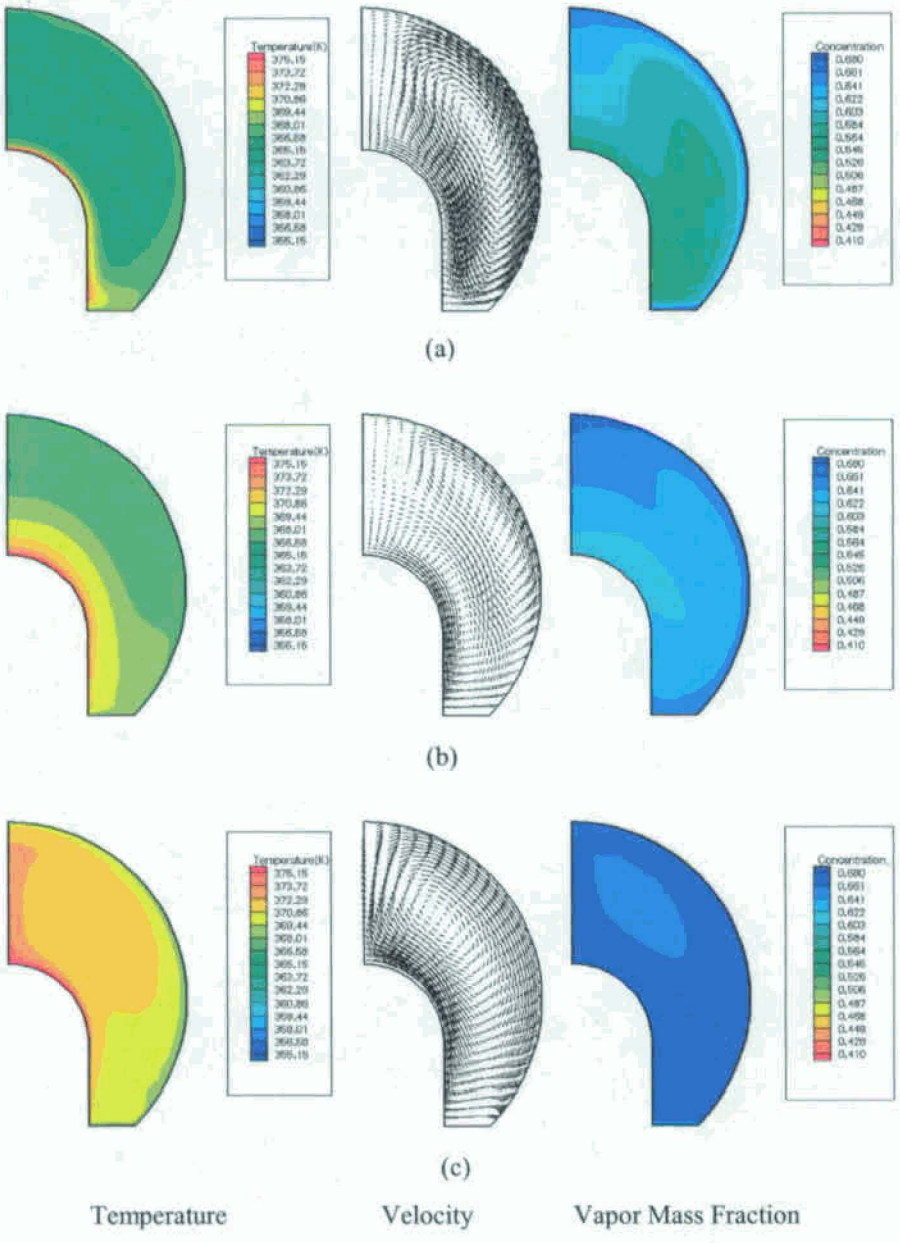

Fig. 3. Temperature, flow velocity, and vapor concentration are plotted at $t = 52$ yr, which is during the repository heat-up phase. Three stages of simulated flow development are shown, including (a) early transient stage with buoyancy ratio N > 1, (b) intermediate transient stage with N ≈ 1, and (c) late quasi-steady-state stage with N < 1.

The transient behavior described above is the byproduct of the manner in which boundary and initial conditions are imposed in the model. For the purpose of this study, the Navier-Stokes model is not run continuously along with the LDTH submodel. Because the initial conditions are based on a Navier-Stokes-model result for an earlier time, they lag behind the evolution of the boundary conditions. Consequently, the simulated transient behavior is the result of the Navier-Stokes model establishing a steady-state temperature distribution and vapor-concentration equilibrium with respect to the new boundary conditions. However, because the thermal evolution of an actual repository system is very slow, we would always expect quasi-steady-state conditions inside the drift.

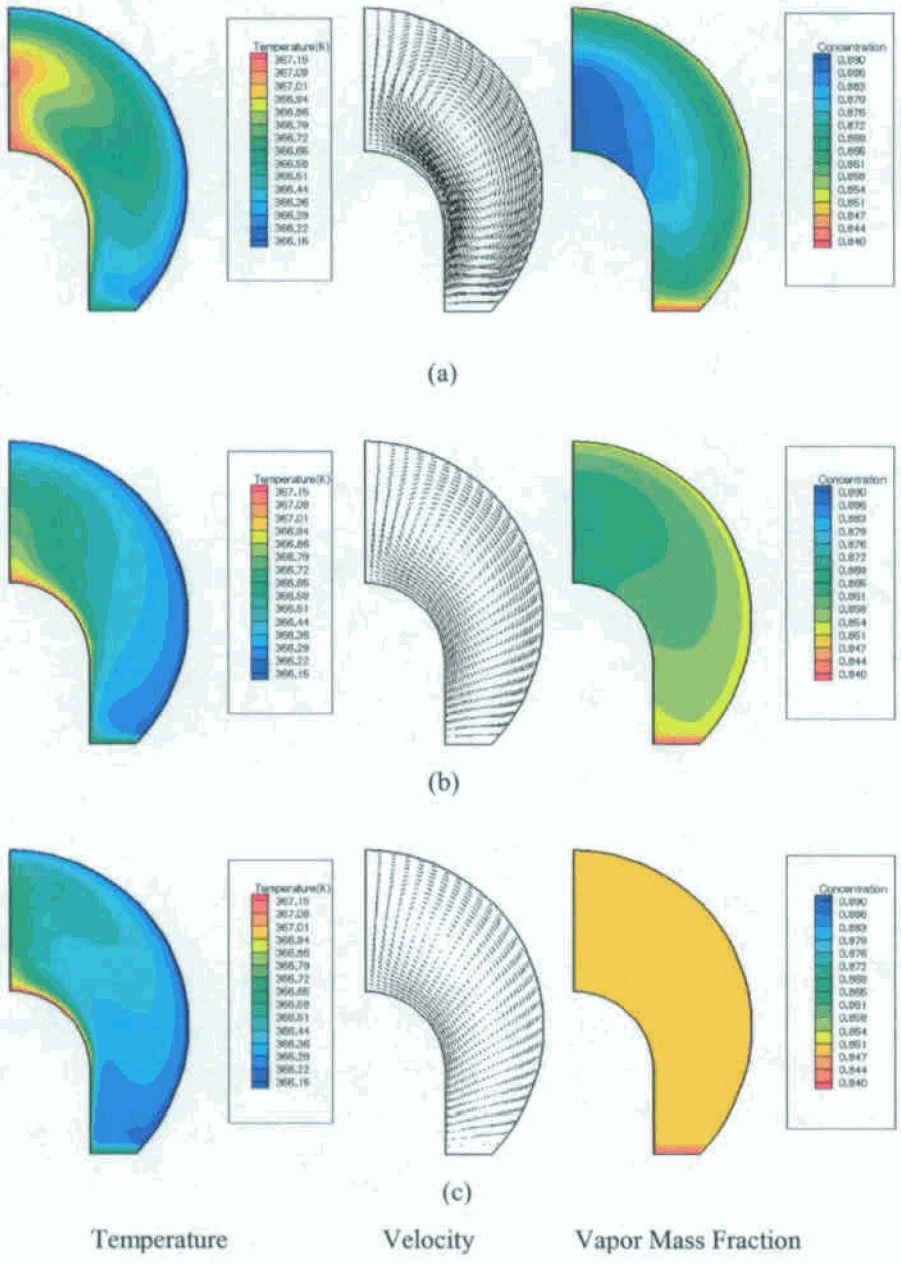

Fig. 4. Temperature, flow velocity, and vapor concentration are plotted at $t = 1400$ yr, which is during the repository cool-down phase. Three stages of simulated flow development are shown, including (a) early transient stage, (b) intermediate transient stage, and (c) late steady-state stage.

III B. Fixed Vapor Concentration on Drip-Shield Surface during Cool-Down Phase

As the repository cools down, if water reaches the outer drip-shield surface, either by dripping or by condensation, a liquid film may exist, which provides a liquid film/gas interface for mass transfer. Under this circumstance, we assign a constant vapor concentration along the drip shield. We assume the liquid film to be very thin and is in thermal equilibrium with drip-shield surfaces. Because of this, no slip boundary conditions are applicable on the drip-shield surface. In addition, the normal velocity is assigned to be zero, which assumes that the mass flow through the drip shield is negligible.

With the above assumptions, constant temperature and vapor-concentration boundary conditions are assigned on the drip-shield surface. For this case, we assign a drip-shield-surface temperature T_{ds} of 94 °C and a vapor-concentration C_{ds} of 0.84, and impose the following temperature and vapor-concentration differences

$$\Delta T = T_{ds} - T_{dw} = 1^{\circ}\mathrm{C}$$

and

$$\Delta C = C_{dw} - C_{ds} = 0.005$$

across the drift. Thus, the assigned drift-wall boundary temperature T_{dw} is 93°C and the assigned boundary vapor concentration C_{dw} is 0.845. Note that the temperature and vapor-concentration gradients are opposing. For this situation, the buoyancy ratio N is estimated to be ~0.74. It is important to note that the purpose of this example is to illustrate the influence of boundary conditions on flow structures within the drift. Therefore, this example may not be representative of a typical waste package at this phase of the thermal evolution of the repository.

For initial conditions, we assign a drift temperature of 93°C, with a vapor concentration of 0.84, which are similar to conditions predicted by the MSTHM LDTH submodel for the cool-down phase. A close inspection of Fig. 5a reveals strong countercurrent circulation patterns existing near the drift wall and drip shield in the early transient stage. This behavior can be understood by considering interactions between opposing thermal and compositional buoyancy effects. The circulation patterns are centered close to the respective drip-shield and drift-wall boundaries, corresponding to where the gradients are steepest. During the intermediate transient stage (Fig. 5b), distinct circulation patterns continue to persist, adjacent to the respective drip-shield and drift-wall boundaries.

A comparison of the velocity profiles in Fig. 5a, 5b, and 5c shows that, after overcoming the influence of the vapor-concentration-gradient effect, the thermal buoyancy effect progressively tends to dominate convective flow, leading to a large central circulation pattern (Fig. 5c). As noted earlier, when $N < 1$, flow is primarily dominated by thermal buoyancy effects.

IV. CONCLUSIONS

We have developed numerical models to investigate double diffusive natural convection within an emplacement drift for a potential nuclear-waste repository in the unsaturated zone. In-drift convective flow and transport behavior is described for both the heat-up and cool-down phases of the thermal evolution of the repository system. During the heat-up phase, or for the case with fixed vapor-concentration on the drip-shield surface, complex unsteady countercurrent flow patterns are observed, which arise from opposing thermal and compositional buoyancy forces. As the drift cools down, thermal buoyancy forces reinforce compositional buoyancy forces, resulting from vapor-concentration gradients, further contributing to the mixing of water vapor within the drift.

Although some of the assumed boundary conditions may not exactly correspond to realistic situations, this study demonstrates the importance of representing both thermal and compositional buoyancy effects in simulating heat and mass transport in drifts. Moreover, insight gained from this study may be helpful in understanding flow and transport phenomena relevant to analogous engineered systems. The results of this preliminary study also support the need for the development of methodologies for coupling CFD models of in-drift thermal-hydrologic (TH) behavior with porous-media models of TH behavior in the adjoining host rock.

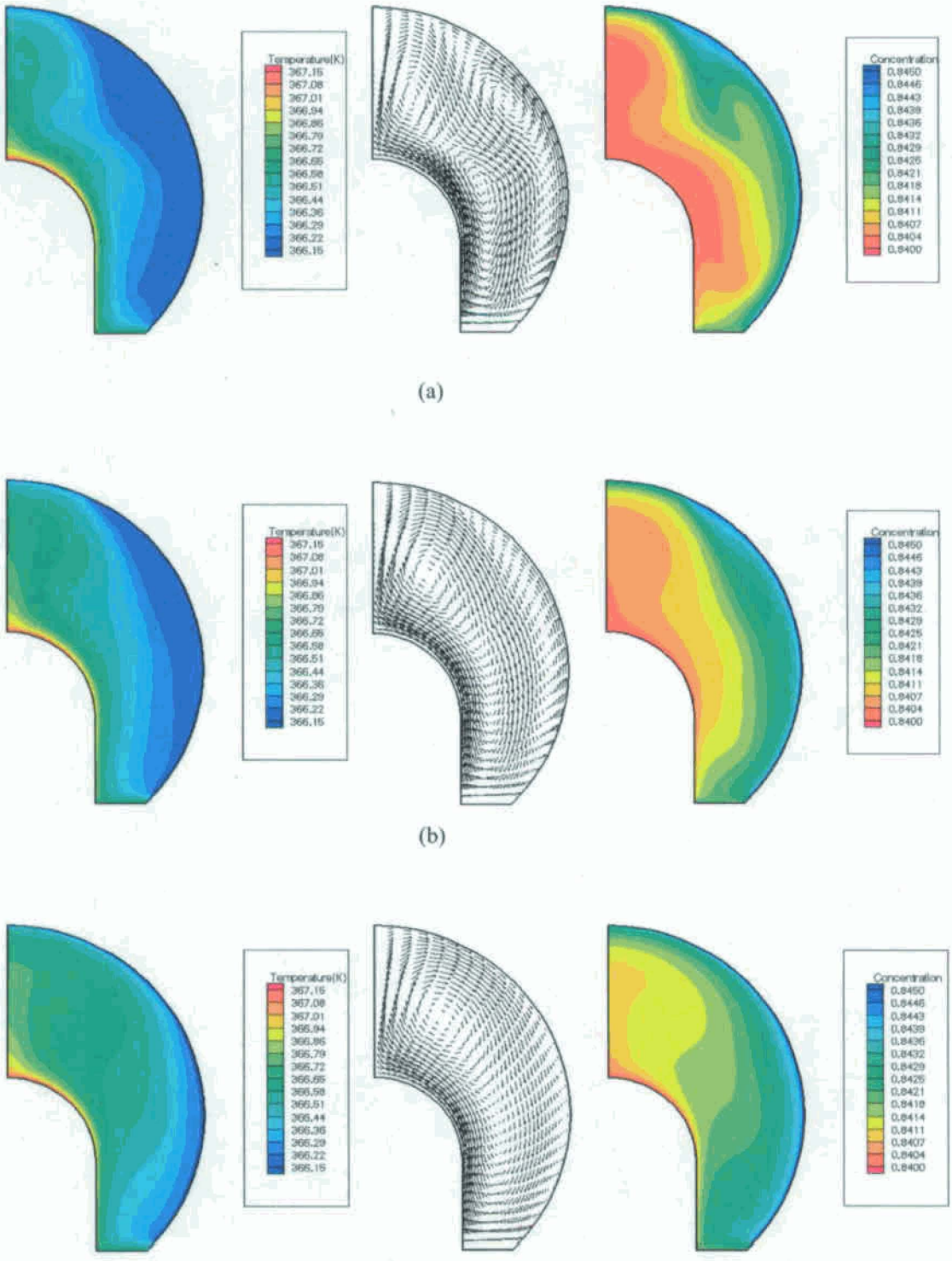

Fig. 5. Temperature, flow velocity, and vapor concentration are plotted at $t = 1400$ yr, which is during repository cool-down phase, with the buoyancy ratio $N \approx 0.74$. Three stages of simulated flow development are shown, including (a) early transient stage, (b) intermediate transient stage, and (c) late steady-state stage.

ACKNOWLEDGMENTS

We gratefully acknowledge the review of Tom Wolery. This work was supported by internal R&D funds at Lawrence Livermore National Laboratory and performed under the auspices of the U.S. Department of Energy by University of California Lawrence Livermore National Laboratory under contract No. W-7405-Eng-48.

REFERENCES

1. V.A.F. COSTA, "Double Diffusive Natural Convection in a Square Enclosure with Heat and Mass Diffusive Walls", *Int. J. Heat Mass Transfer*, **40**, 4061-4071 (1997).

2. C. BÉGHEIN, F. HAGHIGHAT, and F. ALLARD, "Numerical Study of Double-diffusive Natural Convection in a Square Cavity", *Int. J. Heat Mass Transfer*, **35**, 833-846 (1992).

3. BSC (BECHTEL SAIC), In-Drift Natural Convection and Condensation. MDL_EBS_MD-000001, REV 00. Las Vegas, NV (2004).

4. S. W. WEBB, N. D. FRANCIS, S. D. DUNN, M. T. ITAMURA, and D. L. JAMES, "Thermally Induced Natural Convection Effects in Yucca Mountain Drifts", *J. Contam. Hydrol.*, **62-63**, 713-730 (2003).

5. A. BEJAN, "Mass and Heat Transfer by Natural Convection in a Vertical Cavity", *Int. J. Heat and Fluid Flow*, **6**, 149-159 (1985).

6. D.C. WILCOX, *Turbulence Modeling for CFD*, DCW Industries, Inc. (1993).

7. J.J. NITAO, Reference Manual for the NUFT Flow and Transport Code, Version 2.0. Rep. UCRL-MA-130651. Lawrence Livermore National Laboratory, Livermore, CA. (1998).

8. BSC (BECHTEL SAIC), Multiscale Thermohydrologic Model, ANL-EBS-MD-000049 REV 3, Las Vegas, NV (2005).

9. T.A. BUSCHECK, L.G. GLASCOE, K.H. LEE., J. GANSEMER, Y. SUN, and K. MANSOOR, "Validation of the Multiscale Thermohydrologic Model Used for Analysis of a Proposed Repository at Yucca Mountain", *J. Contam. Hydrol.*, **62-63**, 421-440 (2003).

10. T.A. BUSCHECK, Y. SUN, AND Y. HAO, "Multiscale Thermohydrologic Model supporting the License Application for the Yucca Mountain Repository," *Proc. of 2006 International High-Level Radioactive Waste Management Conference*, Las Vegas, NV, April 30 – May 4, American Nuclear Society, LaGrange Park, IL (2006).